

We are IntechOpen, the world's leading publisher of Open Access books Built by scientists, for scientists

6,900

Open access books available

185,000

International authors and editors

200M

Downloads

Our authors are among the

154

Countries delivered to

TOP 1%

most cited scientists

12.2%

Contributors from top 500 universities



WEB OF SCIENCE™

Selection of our books indexed in the Book Citation Index
in Web of Science™ Core Collection (BKCI)

Interested in publishing with us?
Contact book.department@intechopen.com

Numbers displayed above are based on latest data collected.
For more information visit www.intechopen.com



FT-IR Spectroscopy in Medicine

Vasiliki Dritsa

National Technical University of Athens, NTUA
Greece

1. Introduction

Infrared spectroscopy has been widely applied for the characterisation of various substances. Due to its sensitivity to the chemical information and architecture of the molecule, infrared spectroscopy can play an important role in new applications such as in the life-science field and not only in the traditional fields of physics and chemistry. Spectroscopic techniques are simple, reproducible, non-destructive without particular sample preparation. As a result, they provide information for the functional groups, bonds and molecular structure.

Herschel discovered the existence of infrared radiation when he tried to measure the heat produced by separate colors of a rainbow spectrum in 1800. He noted that the highest temperature fell beyond the red end of the spectrum, implying the existence of invisible light beyond the red. Herschel termed this light *calorific rays*. Infrared spectra originate on the vibrational motions of atoms in chemical bonds within molecules. When a beam of light containing the IR radiation band is passed through a sample, light energy from the photons is absorbed by the chemical bonds and excites the vibrational motions. As a molecule absorbs radiation at a specific frequency, it produces a band in the infrared spectrum at the corresponding wavenumber. The approximate position of an infrared absorption band is determined by the vibrating masses and the chemical bonds (single, double, triple). The exact position of the band depends also on electron withdrawing or donating effects of the intra- and intermolecular environment and coupling with other vibrations. The strength of absorption increases with increasing polarity of the vibrating atoms. The modes of vibration in a molecule that can absorb infrared radiation are many and increase with increasing complexity of the molecule. The vibrations that contribute to the spectrum are bending and stretching vibrations between atoms and rocking, twisting and wagging of a functional group (Theophanides, 1984; Goormaghtigh et al., 1999).

Fourier transform infrared spectroscopy is preferred over dispersive or filter methods of infrared spectroscopy due to the sensitivity and the rapid data collection. The FT-IR spectrometer uses an interferometer to modulate the wavelength from a broadband infrared source. Light emitted from the infrared source is split by a beam splitter. Half of the light is reflected towards a fixed mirror and from there reflected back towards the beamsplitter where about 50% passes to reach the detector. The other half of the initial light intensity passes the beam splitter on its first encounter, is reflected by the moving mirror back to the beamsplitter where 50% of it is reflected towards the detector (Figure 1). When the two

beams recombine, they interfere and there will be constructive or destructive interference depending on the optical path difference. A detector measures the intensity of transmitted or reflected light as a function of its wavelength. The signal obtained from the detector is an interferogram, which is analyzed by a computer using Fourier transforms to obtain a single-beam infrared spectrum (Barth, 2007).

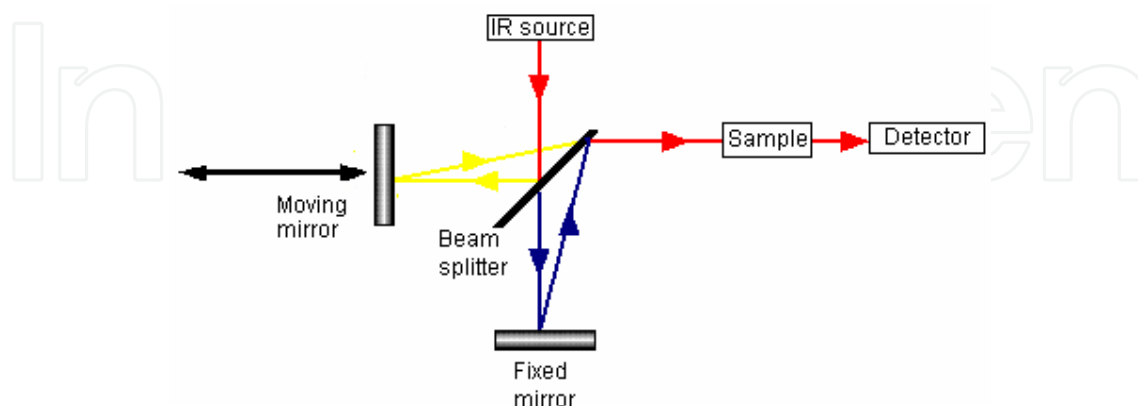


Fig. 1. Schematic function of an FT-IR set-up.

Fourier transform infrared (FT-IR) spectroscopy has proven to be a fundamental and valuable technique in biology and medicine due to its high sensitivity to detecting changes in the functional groups belonging to tissue components such as lipids, proteins and nucleic acids. Each of these tissue components can be detected and characterized by their characteristic absorption bands at specific wavelengths within a single spectrum. For biological spectroscopy, the important vibrations occur in the mid-infrared region (4000 to 400 cm^{-1}) where most organic molecules show characteristic spectral features (Theophanides, 1978). The domain of biological applications of infrared spectroscopy encompasses a wide range of very different molecular structures. Biological molecules are categorized into proteins, nucleic acids, lipids, membranes, blood tissues. Different biomolecules interact among themselves, comprising electrostatic interactions, hydrogen bondings and van der Waals interactions, which can be readily studied by infrared spectroscopy.

For complex samples that transmit infrared radiation poorly or no changes must take place in their specimen, attenuated total reflection (ATR) is applied. The technique was developed by Harrick (1960) and Fahrenfort (1961). ATR is a specialised sampling technique, where the sample is placed on ATR crystal. An infrared beam is passed through the ATR crystal, reflects off the interface of the crystal and the sample, and is passed through to the detector. During the reflection, an evanescent wave extends beyond the crystal into the sample, which enables the absorption of energies corresponding to infrared frequencies by the sample. The penetration depth of the evanescent wave is a function of wavelength with deeper penetration at longer wavelengths. This may lead to distortions in the relative intensities of infrared peaks if sample thickness is insufficient for complete coverage of the evanescent wave (Goormaghtigh et al., 1999). Figure 2 shows the diagram of a basic ATR set up.

Attenuated total reflection (ATR) coupled with FT-IR, can obtain the infrared spectrum of solid or liquid samples in their native state. The resultant FT-IR spectra provide molecular information of samples. Samples with minimal size can be non-destructively analyzed,

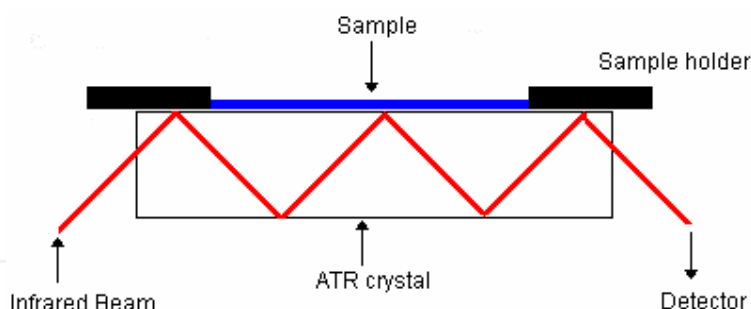


Fig. 2. Diagram of the ATR setup.

particularly in the biomedical sciences. High quality spectra can be obtained from cell suspensions containing 10-50,000 cells, depending upon the size of the cells. In the case of tissues, such measurements generally require a sample size of 1 mm³ (Legal, 1991). Additionally, ATR has been established as a method of choice of analyzing samples that are either too thick or too strongly absorbing to analyse by other transmitting techniques. The use of these techniques have become a great potential over other diagnostic methods for the determination of the chemical components of tissues at various diseases states, due to the rapid and reagent free procedure. An advantage of ATR-FTIR to study the structure of biomembranes is that the membrane can be deposited on the surface of the internal reflection element (IRE) as a thin film of highly oriented membranes by evaporation of the water. Variations in spectral signatures arising from nucleic acids, proteins and lipids can provide important information in a number of disease states.

1.1 Medical applications of FT-IR spectroscopy

In 1949 Blout, Mellors and Woernley in 1952 reported that infrared spectra of human and animal tissues could provide information on the molecular structure of tissues. These studies met with limited success due to non-developed instrumentation available and little knowledge of spectroscopic properties of biological molecules and the complexity of the samples. At the same time, Elliot and Ambrose (1950) proposed empirical correlations between peptide structure and the Amide I and Amide II bands. The development of sensitive and high throughput spectrometers led to a wide field of medical applications of FT-IR spectroscopy. The rapid experimental and theoretical development took place in 1970s, where Fourier Transform interferometers interfaced to digital computers.

FT-IR has been extensively applied for the determination of a biochemical metabolite in biological fluids. The improved sensitivity and data processing capability of new instruments, the presence of water is no longer a serious obstacle in the analysis of fluids. Current enzymatic methods require frequent calibration controls and reagents, and this is very costly. FT-IR spectroscopy has been used for the determination of glucose, total protein, urea, triglyceride, cholesterol, chylomicron and very low density lipoproteins in plasma and serum, in order to replace commonly used ultracentrifugation techniques (Deleris and Petibois, 2003; D. Krilov et al., 2009). The differences in the size, lipid composition and apolipoprotein structure in particular classes of lipoproteins are reflected in the characteristic spectral bands of lipid and protein moiety.

FTIR has received much attention as a promising tool for non-destructive characterisation of the molecular features of atherosclerosis due to the fact that vibrational spectra are sensitive

to structures of biological molecules and their changes with the diseased state. Additionally, FTIR-spectroscopy on biological samples was pioneered in the medical sciences where it is used as a clinical tool to distinguish between malignant and healthy human cells. Acquired spectra of cells/ tissues give a detailed biochemical fingerprint that varies dependent on the clinical status. It has been successfully applied in the study of various human tissues such as mineralized tissue (Kolovou and Anastasopoulou, 2007), skin (McIntosh, 1999), colon (Conti et al., 2008), breast (Anastassopoulou et al., 2009), arteries (Mamarelis et al., 2010), cartilage (Petra et al., 2005), the urinary tract (prostate, bladder) (Gazi et al., 2003), lung (Yano et al., 2000), liver (Li et al., 2004), heart and spleen (Chua-anusorn and Webb, 2000; Gough et al., 2003).

According to a wide range of studies, it has been proved that FT-IR spectroscopy has been a significant clinical technique, which provides detailed information of the chemical components of the tissues (proteins, lipids, carbohydrates, DNA). By analysing chemical and biochemical changes, specific spectral features are to be considered for a diagnostic evaluation. In this chapter, it is discussed FT-IR spectroscopy in the field of atherosclerosis in carotid and coronary arteries. Experimental studies are summarized demonstrating the possibilities and prospects of these methods to detect and characterize the disease.

1.2 Atherosclerosis

Atherosclerosis, the most common form of cardiovascular diseases, is a leading cause of death affecting almost one third of humans in developed countries. Atherosclerosis is the usual cause of heart attacks, strokes, and peripheral vascular disease. Ross and Glomset (1973) were the first who introduced that atherosclerosis forms as a result of damage of endothelium. Multiple factors contribute to atherosclerosis, such as hypertension, smoking, diabetes mellitus, obesity, hypercholesterolemia and genetic predisposition. The major characteristics of human atherosclerosis are based on studies of coronary and carotid artery lesions. Atherosclerosis is a chronic inflammatory disease characterised by a stenotic lesion of arterial walls. Atherosclerotic lesions can cause stenosis with potentially lethal distal ischemia or can trigger thrombotic occlusion of major conduit arteries to the heart, brain, legs and other organs. The extracellular and intracellular accumulation of lipids from the circulating blood results in the thickening of the inner layer of the arterial wall. Analyses of human lesions by modern computer methods and biomechanical testing have established the probable link between this characteristic morphology and the actual rupture event (Lee and Libby, 1997).

During atherogenesis, the structure of the arterial wall changes in the intimal layer. The disease process consists of the intimal smooth muscle cell proliferation, the formation of large amounts of connective tissue matrix by the proliferated smooth muscle and the deposition of lipids within the cells and in the connective tissues surrounding them.

In the early stages of atherogenesis, fatty deposition occurs.

Atherogenic lipoproteins such as low-density lipoproteins (LDLs) enter the intima, where they are modified by oxidation or enzymatic activity and aggregate within the extracellular intima. Monocytes are transformed into macrophages, take up lipoproteins and become foam cells. The accumulation of foam cells leads to the formation of fatty streaks, which are often present in the aorta of children, the coronary arteries of adolescents, and other

peripheral vessels of young adults (Steinberg and Witztum, 1999). Fatty streaks are widely considered to be the initial lesion leading to the development of complex atherosclerotic lesions (Figure 3). The progression requires an additional stimulus, i.e. risk factor for the development of atherosclerosis. Smooth muscle cells secrete extracellular-matrix components (proteoglycans), increasing the retention and aggregation of lipids to monocytes (Stary, 1994).

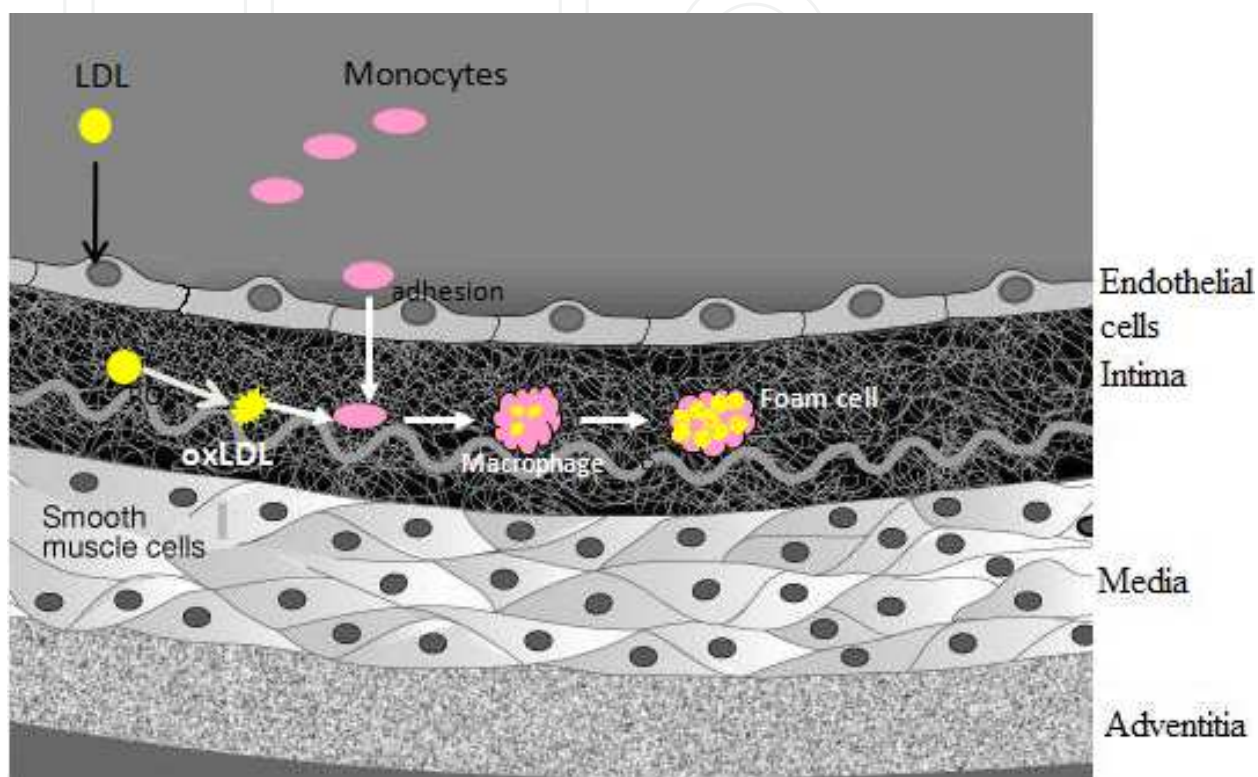


Fig. 3. Formation of atherosclerotic plaque.

1.3 Study of atheromatous plaques by FT-IR

Atherosclerosis is a complex process and the behaviour of vulnerable atherosclerotic plaques is believed to be closely related to plaque composition. Knowledge of the composition and physical chemistry of atherosclerotic plaques is essential for understanding how these plaques originate and mature and how reversal of the pathological process may be achieved (Insull, 2009). It is therefore important to develop an effective technique for examining plaque constituent properties. FT-IR provides information on the molecular and structural composition directly in the untreated, unfixed, and unstained whole tissue, thus preserving the integrity of the original cells. In this work, Fourier transform infrared spectroscopy using attenuated total reflectance (FTIR-ATR) has been used to assess and analyze the biochemical properties of human atherosclerotic plaques. Additionally, Scanning electron microscopy (SEM) has been used to provide valuable information on the general characteristics of the morphology and structure of carotid and coronary arteries. SEM allows the scanning of large area in the atheromatous plaque and the use of large magnification provides a detailed view. Human tissues were viewed directly without any conductive coatings.

2. Materials and methods

20 samples from carotid and coronary arteries from patients (60-85 years old) who underwent endarterectomy were used for the study (Figure 4). Representative sections of the Carotid atheromatic plaques and coronary arteries were restored in formalin. The FT-IR spectra were obtained with a Nicolet 6700 thermoscientific spectrometer, connected to an attenuated total reflection, ATR, accessory. For each region a series of spectra were recorded and every spectrum consisted of 120 co-added spectra at a resolution of 4 cm^{-1} and the OMNIC 7.1 software was used for data analysis. All the spectra for each patient and region were obtained in the same way. The analysis of bacterial morphology was performed by Scanning Electron Microscopy –SEM using a Fei Co at an accelerating potential 25 kV. Uncoated freeze dried cells were examined with LFD and BSED detectors. Qualitative elemental data analysis of the samples was determined by EDX (Energy-dispersive X-ray spectroscopy).



Fig. 4. Sample from carotid artery A: atheromatous plaque, B: adventitia, C: intima

3. Analysis and discussion of FT-IR spectra

Two representative FT-IR absorption spectra of a carotid and coronary artery in the region $4000-400\text{ cm}^{-1}$ are shown in Figure 5. The spectra provide distinct features for the determination of the chemical composition and the diagnostic classification of arterial wall.

The spectra in high frequency region, $4000-2500\text{ cm}^{-1}$, mainly consist of νOH , νNH , asymmetric and symmetric methyl (CH_3) and methylene (CH_2) stretching vibrations. Significant differences are observed among carotid and coronary artery. In the case of coronary artery, the shoulder observed at 3524 cm^{-1} is assigned to νOH vibration of hydroxyl groups produced by the hyperoxidation of lipids and proteins and by addition of hydroxyl (HO^\bullet) free radicals to the double bonds of the fatty acids. The band at 3282 cm^{-1} is assigned to νNH stretching of the peptide bond ($-\text{NHCO}-$) of proteins (Theophanides et al., 1988). According to the intensity of νNH band, it is estimated that the coronary artery has a higher damage in proteins compared to the carotid artery.

The olefinic band $\nu=\text{C-H}$ at 3077 cm^{-1} arises from the unsaturated lipids. In coronary artery, the high intensity of the band indicates that the foam cells are rich in low density lipoproteins (LDL). It is known that unsaturated lipids are more prone to lipid peroxidation (Mamarelis et al., 2010). The integrated area of the olefinic CH band can be used as an index of relative concentration of double bonds in the lipid structure from unsaturated fatty acyl

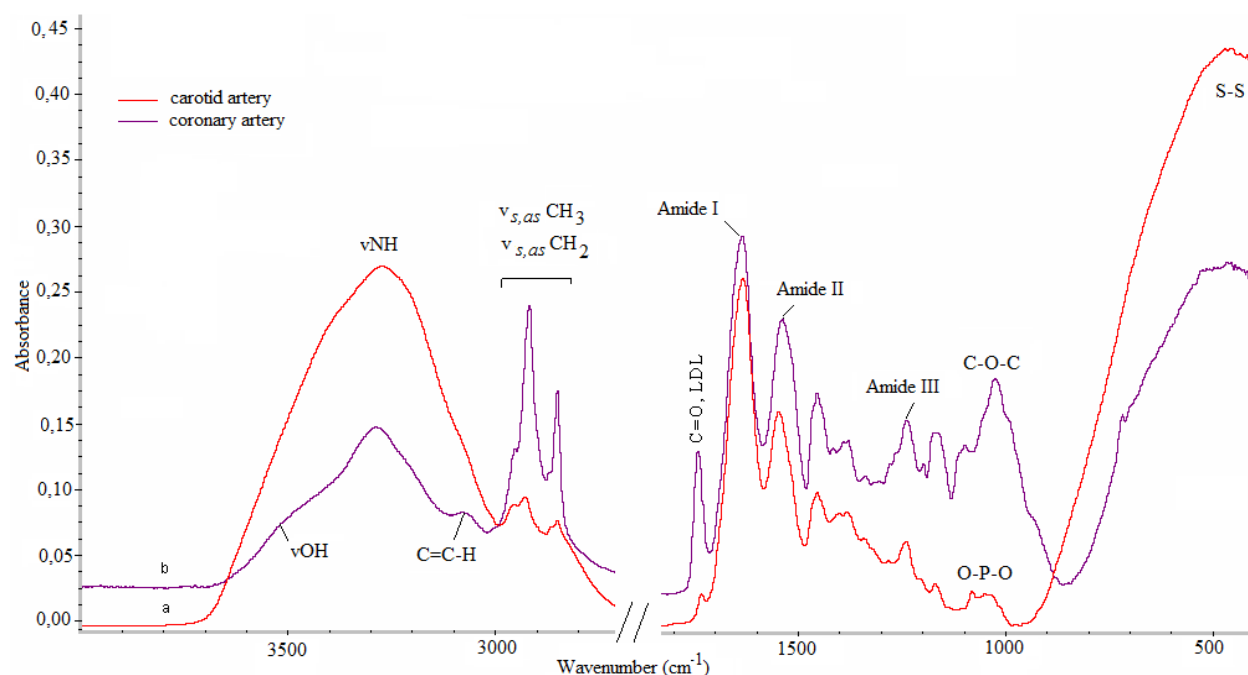


Fig. 5. FT-IR adsorption spectra obtained from human tissues (a) carotid artery, (b) coronary artery in the region of 4000-400 cm^{-1} .

chains (e.g. linolenic, arachidonic, etc.), and/or due to lipid peroxidation. For this reason, the intensity of this band can be used as a diagnostic band of LDL.

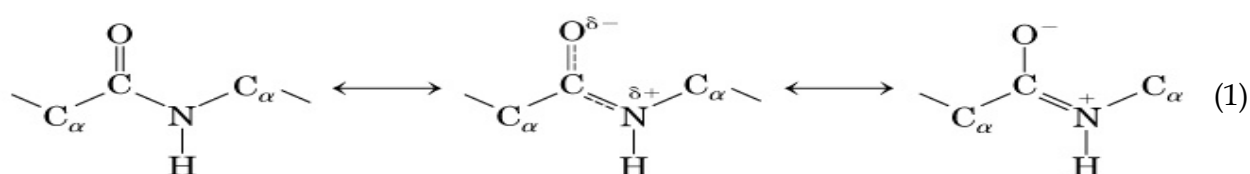
The CH_2 asymmetric (2929 cm^{-1}) and symmetric (2851 cm^{-1}) stretching vibrations give intense bands, while asymmetric CH_3 stretching at 2955 cm^{-1} and symmetric stretching at 2865 cm^{-1} bands are seen as shoulders. The bands arise from lipids, phospholipids and membranes. The intensity of symmetric and asymmetric stretching vibrations of CH_2 and CH_3 reflect lipid hyperoxidation (Liu et al., 2002). The increase in the intensity of the bands in coronary artery shows that the environment is less lipophilic due to fragmentation of the lipoproteins and accumulation of free cholesterol and cholesterol esters in the atheromatous core, as a result membrane fluidity changes significantly (Anastassopoulou and Theophanides, 1990).

Significant changes are also observed in the infrared absorption bands in the region $1800\text{--}1500 \text{ cm}^{-1}$, as it is shown in the spectra. The presence of cholesterol esters and other ester-containing compounds is also identified from the carboxyl ion ($-\text{O}-\text{C}=\text{O}$) stretching absorption at 1735 cm^{-1} apart from the $\text{C}=\text{C}-\text{H}$ stretching band (3077 cm^{-1}). This band confirms lipid hyperoxidation and the increased intensity of the band indicates increased LDL concentrations according to the blood analyses of the patient. All the patients who underwent coronary endarterectomy showed higher intensity in the specific band. The bands at 1735 and 3077 cm^{-1} can be used as indicators for LDL cholesterol of patients.

The Amide I absorption band, arises mainly from the $\text{C}=\text{O}$ stretching vibration with minor contributions from the out-of-phase CN stretching vibration, the CCN deformation and the NH in-plane bend. The Amide I band is down-shifted near 1635 cm^{-1} , approximately 20 cm^{-1} difference compared to the absorption of a normal tissue (1656 cm^{-1}), suggesting a

conformational change in α -helices (Anastassopoulou et al., 2009). The shifting of the Amide I band suggests that proteins lose their structure from α -helix to random coil due to fragmentation induced from free radical reactions. The exposure of proteins to free radicals induces secondary structural changes, since secondary structure is stabilized by hydrogen bonding of peptide backbone. Proteins are organized into α -helices, but the hydrogen bond is damaged, so the chains opens and are more prone to free radicals, leading to the change of α -helix to random coil.

The change of dipole moment of peptide bond, as it is shown in equation [1] at resonance structures, leads to a change in the orientation of amino groups (NH) to the carbonyl group C=O, resulting in the destruction of α -helix and the secondary structure of proteins.



The band at 1537 cm^{-1} is attributed to the vibrations of Amide II. The amide II mode is the out-of-phase combination of the NH in plane bend and the CN stretching vibration with smaller contributions from the CO in plane bend and the NC stretching vibrations. The bands of Amide I and Amide II are representative of ---NH---CO--- vibrations of proteins (Theophanides et al., 1988). The analysis of the spectra by Fourier self-deconvolution was used to enhance resolution in the region $1800\text{--}1500\text{ cm}^{-1}$ (figure 6 and 7).

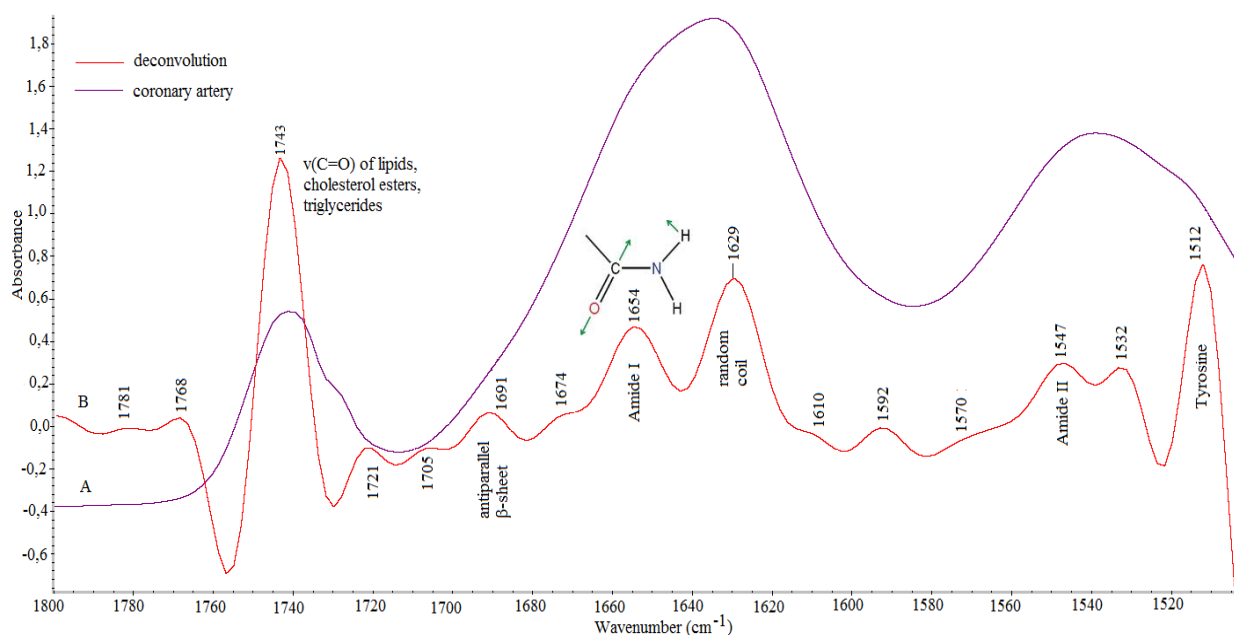


Fig. 6. A: FT-IR spectra of coronary artery in the region $1800\text{--}1500\text{ cm}^{-1}$, B: Deconvolution of the spectra in the same region.

As it is determined from the deconvolution in the spectra of the coronary artery of a patient, the band at 1781 and 1768 cm^{-1} is attributed to the carboxyl anions ---COO--- of the

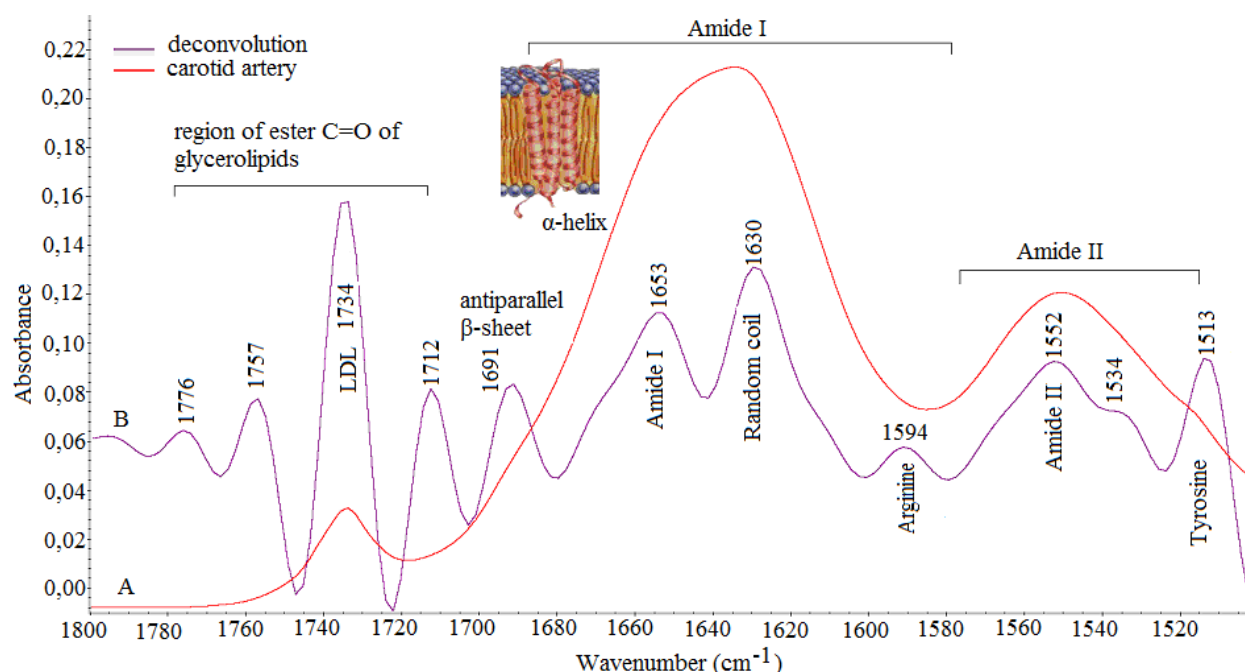


Fig. 7. A: FT-IR spectra of carotid in the region 1800-1500 cm^{-1} , B: Deconvolution of the spectra in the same region.

atheromatous plaque, which are probably connected to metal with high molecular weight. The broad band in the region 1750–1720 cm^{-1} appears to be the summation of two underlying components by deconvolution, giving one band at 1743 cm^{-1} and a second one at 1721 cm^{-1} . These bands are assigned to LDL cholesterol and are due to stretching vibrations of the carbonyl group involved in ester bonds. These bands arise from the interfacial region of the glycerolipid moiety and are responsive to changes in their environment, such as hydrogen bonding or polarity (Arrondo and Goni, 1998).

The broad band at 1700–1600 cm^{-1} is Amide I band, constituted from the bands at 1691, 1674, 1654, 1629, and 1610 cm^{-1} . The main amide I band at 1654 cm^{-1} is indicative of a high content of α -helical structure, although part of the absorption at this frequency also corresponds to random coil structure at 1630 cm^{-1} and antiparallel β -sheet at 1691 cm^{-1} (Barth, 2007). Particularly, the band at 1691 cm^{-1} arises from the peptide bond of proteins and mainly from the vibration of C=O compared to NH group. The band at 1674 cm^{-1} is attributed to apolipoprotein ApoC-III, which resides in HDL and inhibits the lipolysis of triglyceride-rich lipoproteins. The decrease of α -helix absorbance band compared to random coil confirms the fragmentation due to free radical interactions.

The bands at the wavelengths 1592, 1570, 1547 and 1512, which are assigned to the groups of arginine, aspartic acid, glutaminic acid and tyrosine of apolipoproteins Apo A-I. The specific bands were revealed after the deconvolution treatment of spectra. The wide band at 1537 cm^{-1} is split into two bands, one in 1550 cm^{-1} , which is characteristic of Amide II absorption due to the stretching vibrations C-N and bending vibration N-H because of the influence of lipids. The apolipoproteins of Apo A-I and A-II, are components of HDL (High density Lipoproteins) and control HDL metabolism (Nara et al., 2002). The distinctive structures and properties of apoA-I and apoA-II, the two major HDL proteins, determine in different ways the thermodynamic stability of HDL - the former through its greater plasticity and the latter by its higher lipophilicity. Apo A-I protects phospholipids from oxidation due to a

conformational constraint governed by adjacent amphiphatic α -helices located in C-terminal lipid-binding domain. Apo A-I is a potent inhibitor of lipid peroxidation, protecting the phospholipids from water-soluble and lipophilic free radical initiators (Bolanos-Garcia and Miguel, 2003). The reduction of Apo A-I and A-II and the increase of the characteristic band of LDL at 1735 cm^{-1} are connected to the blood analyses of the patients.

Relatively, the deconvolution in the carotid artery spectra of a patient as it is shown in figure 7, revealed the bands at 1776 and 1757 cm^{-1} , which are attributed to the carboxyl anions COO^- of the atheromatous plaque. The lipid content is indicated by the lipid ester band at 1734 cm^{-1} . The wide band of amide I is split to the bands at 1691 , 1653 , 1630 cm^{-1} , which reveals the destruction of α -helical structure of proteins due to the free radicals reactions. The peptide bond appears another characteristic band at the region of amide II absorption, which is constituted from the bands at 1592 , 1552 , 1534 and 1513 , which are attributed to arginine, α -helix of collagen, random coil and tyrosine.

In carotid and coronary artery, the deconvolution confirmed the peroxidation of lipids and lipoproteins. The intensity of the aldehydes due to peroxidation of LDL (1735 and 1742 cm^{-1}) is higher in the case of coronary artery. Various small molecular weight aldehydes such as acrolein, malondialdehyde (MDA), and 4-hydroxy-2-nonenal (HNE) are formed during lipid peroxidation as secondary or decomposition products. The main product of aldehydes in this region is malonaldehyde (MDA), which is an end product of lipid peroxidation that starts with abstracting a hydrogen atom from an unsaturated fatty acid chain, and this peroxidation spreads to the adjacent fatty acids continually. It has been proved that MDA inhibits the metabolism of high density lipoproteins (HDL), which are protecting factors of human organism. Thus, the increase of LDL, which is relative to the clinical condition of the patients, is associated with a higher risk of cardiovascular disease.

In figure 8, the wide band at 1454 cm^{-1} is constituted of two bands at 1461 cm^{-1} and 1443 cm^{-1} in the coronary artery, which arise from the carbon chain of lipids, combination of bending vibrations of δCH_2 of carbon chains of lipids and δCOOH of non-ionic groups, respectively. The deconvolution of the band in the carotid artery revealed three bands, at 1467 , 1454 , 1443 cm^{-1} , which are assigned to the bending vibrations of $\delta_{\text{as}}\text{CH}_3$ of lipids, stretching vibration of νCO_3^{2-} and δCOOH of non-ionic groups, respectively. In the coronary artery, the intense increase of the band results in the decrease of lipophilic environment of membrane. This observation is in agreement with the increase of the stretching vibration bands in the region $3000\text{--}2870\text{ cm}^{-1}$.

The absorptions at 1238 , 1173 and 1024 cm^{-1} matched the spectral patterns that arise from amide III (in plane N-H bending and C-N stretching vibrations) and the asymmetric and symmetric stretching modes of PO_2^- in DNA or the phosphodiester groups of the phospholipids, cholesterol ester and C-O-C vibrations of fatty acids and ketals (Mamarelis et al., 2010), respectively, which are product of atheromatous plaque of coronary and carotid artery due to hyperoxidation of membranes (Figure 9). The comparison of coronary and a carotid artery reveals that intense hyperoxidation has taken place in the coronary artery, as it is determined from the C-O-C vibrations of aldehyde groups. To the contrary, the vibrations of phosphate groups PO_2^- of phospholipids and DNA band together with the bending vibration $\nu_4\text{CO}_3^{2-}$ at 874 cm^{-1} suggests that the atheromatic plaque is consisted from calcium carbonate (CaCO_3) and that the foam cells are rich in calcium minerals (Petra et

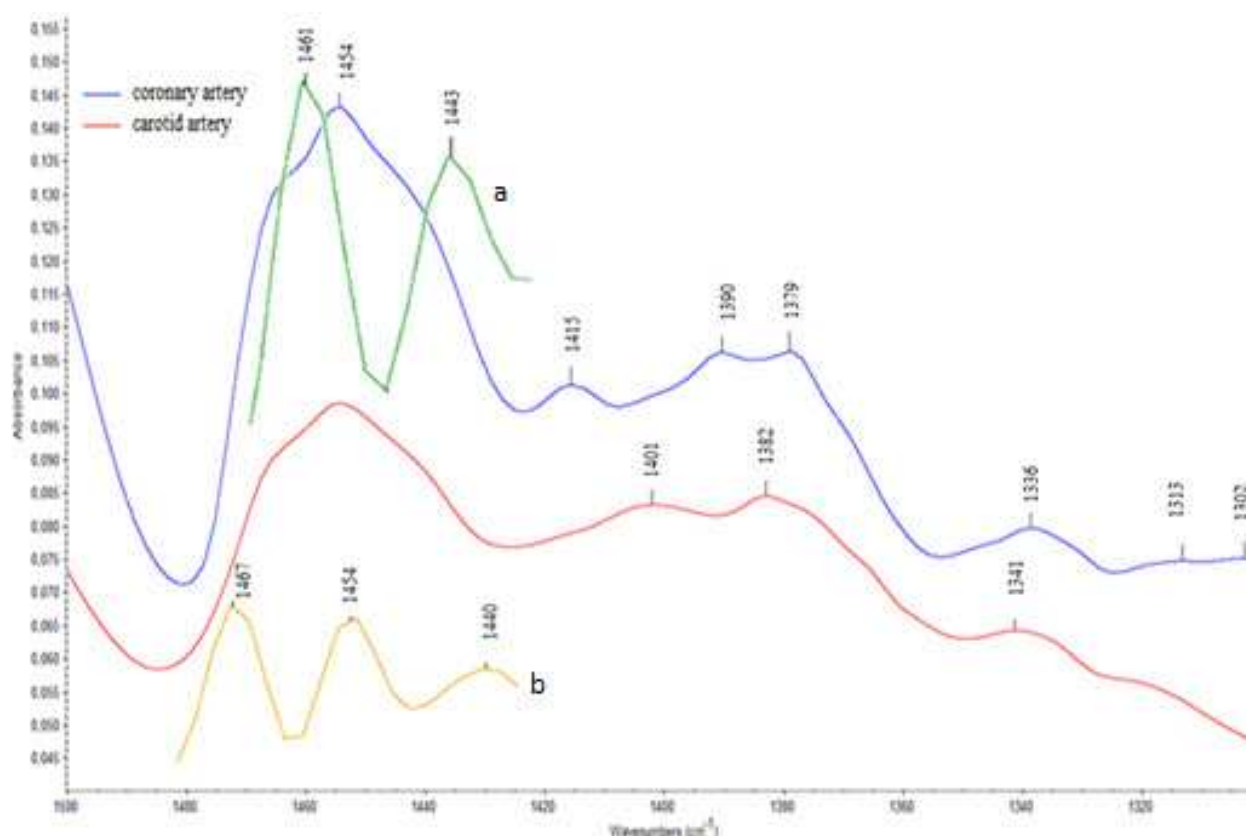


Fig. 8. FT-IR spectra of carotid and coronary artery in the region 1500-1300 cm^{-1} and the deconvolution of the band at 1454 cm^{-1} of coronary (a) and carotid (b) artery.

al., 2005). The calcified atherosclerotic plaque spectra are dominated by bands from calcified minerals such as hydroxyapatite and carbonated apatite.

4. Scanning electron microscopy

Scanning electron microscopy (SEM) was used for imaging biological specimens, thus enabling rapid and high-resolution imaging of atherosclerotic lesions (Kamar et al., 2008). High resolution images can be obtained without gold coating, thereby enabling imaging of atherosclerotic lesions close to its original state. Significant structural alterations and mineral salts were observed in carotid and coronary arteries. The membrane morphology of carotid artery is shown in figure 10.

The architecture of foam cells is heterogenous as well as the size of white stones. It was found that this region is rich in phosphorous. It has been found that initiation of atheromats takes place in this region and thus, it is expected to be a region, which corresponds to atheromatic plaque rich in phospholipases (Lp-PLA2). The enzyme Lp-PLA2 hydrolyses the oxidized phospholipids to lysophosphatidyl choline and causes to atherogenesis (Gorelick, 2008; Parthasarathy et al., 2008). The ratio of $[\text{Ca}]/[\text{P}]$ according to elemental analysis (EDAX) demonstrates that the stones of carotid are hydroxyapatite.

On the contrary, the coronary artery is rich in calcium but no phosphorus was detected (Figure 11). As a result, carbonated apatite is mainly formed in coronary arteries. This observation is in agreement with the results from FT-IR spectra. Many of the mineral salts

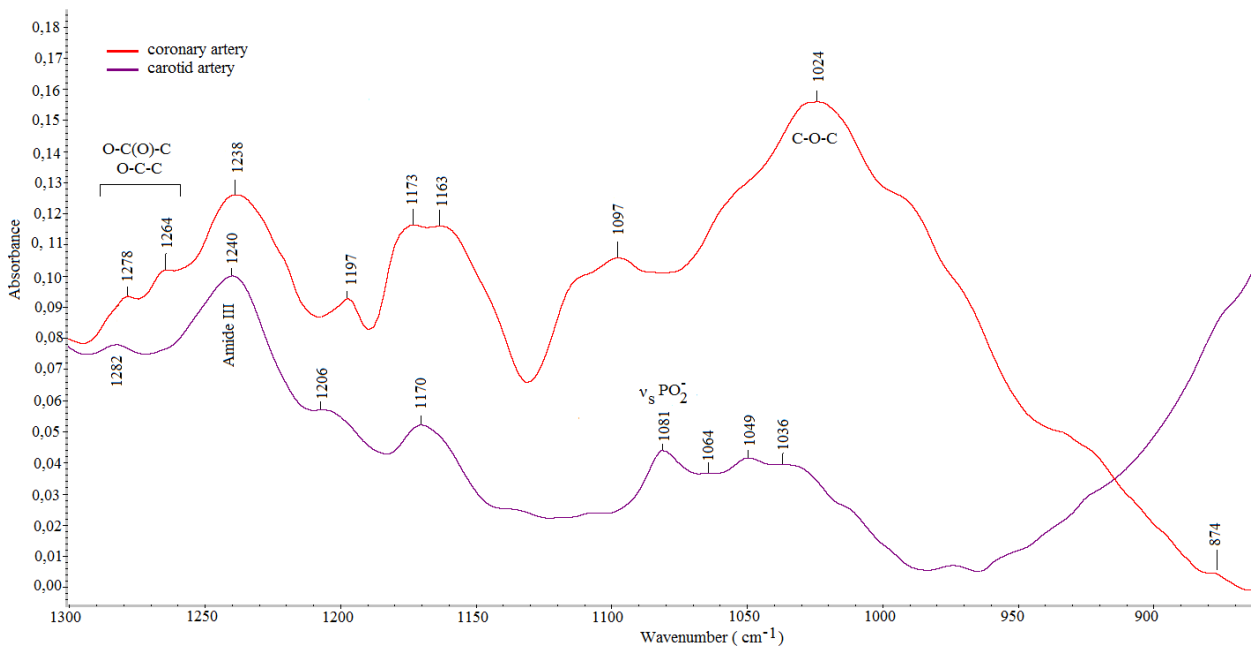


Fig. 9. FT-IR spectra of carotid and coronary artery in the region 1300-800 cm⁻¹.

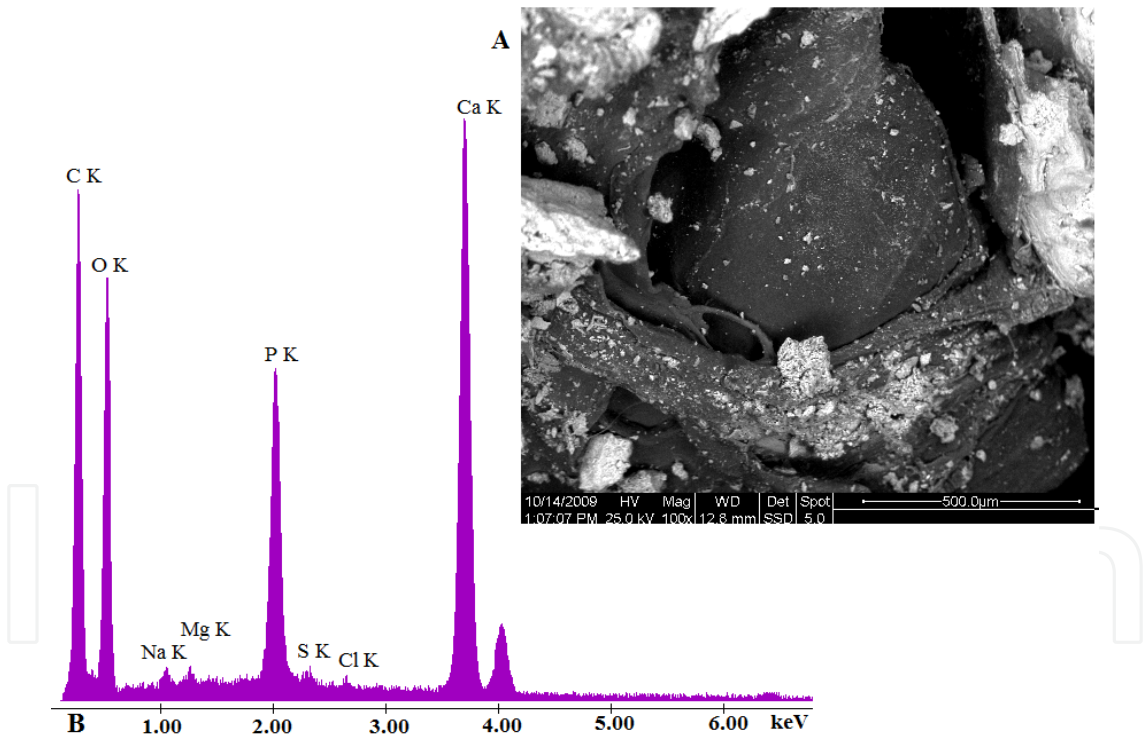


Fig. 10. A:SEM imaging of carotid membrane, region rich in mineral deposits (scale 500 μm), B: EDAX analysis of a white spot.

are not connected to the tissues while other are bound by chemical bonds. Additionally, an increased number of fibrils are presented that confirm the fact that free radicals play an important role in the development of atheromas. The architecture of surface is rich in spheres of LDL, as it was demonstrated from FT-IR spectra. The molecules of LDL obtain the shape of sphere that corresponds to the minimum energy.

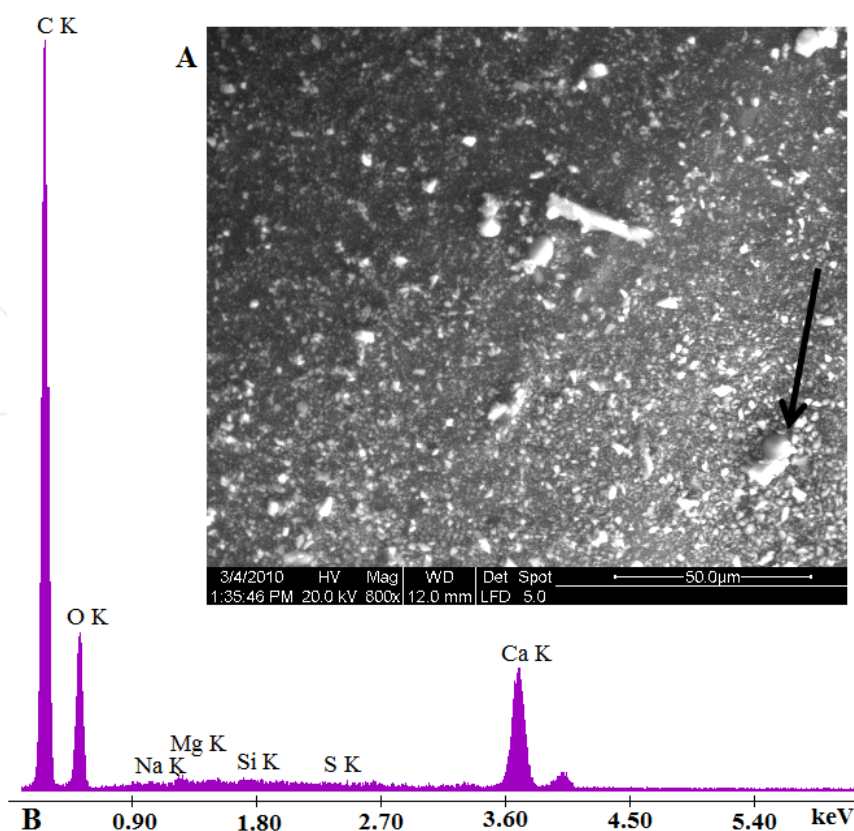


Fig. 11. A: SEM imaging of coronary membrane, region rich in mineral deposits (scale 50 μm), B: EDAX analysis of a white spot.

5. Oxygen-centered free radicals

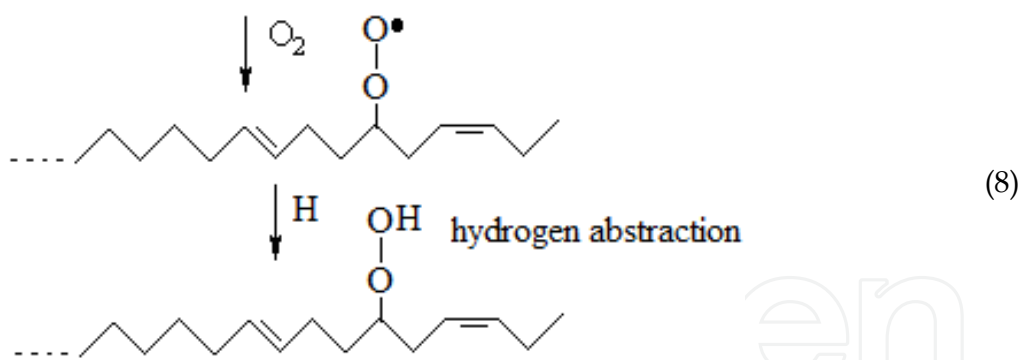
The ubiquitous presence of oxygen in higher species and diatomic oxygen's ability to readily accept electrons has made oxygen-centered free radicals the most frequently encountered radical species, which are involved in the pathogenesis of atherosclerosis. The hydrogen peroxide molecules are intermediate products in the catalytic cycle of oxidation of P₄₅₀ cytochrome according to the reaction [2]:



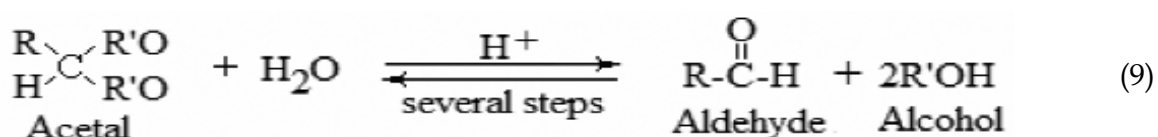
The main factors for the production of free radicals are the iron cations (Fe²⁺) of the hemoproteins and bivalent copper cations (Cu²⁺) from copper proteins (Halliwell & Gutteridge, 2000; Anastassopoulou & Dovas, 2007). The iron cations react with hydrogen peroxide and produce hydroxyl free radicals (·OH), according to Fenton or Haber-Weiss like reactions:



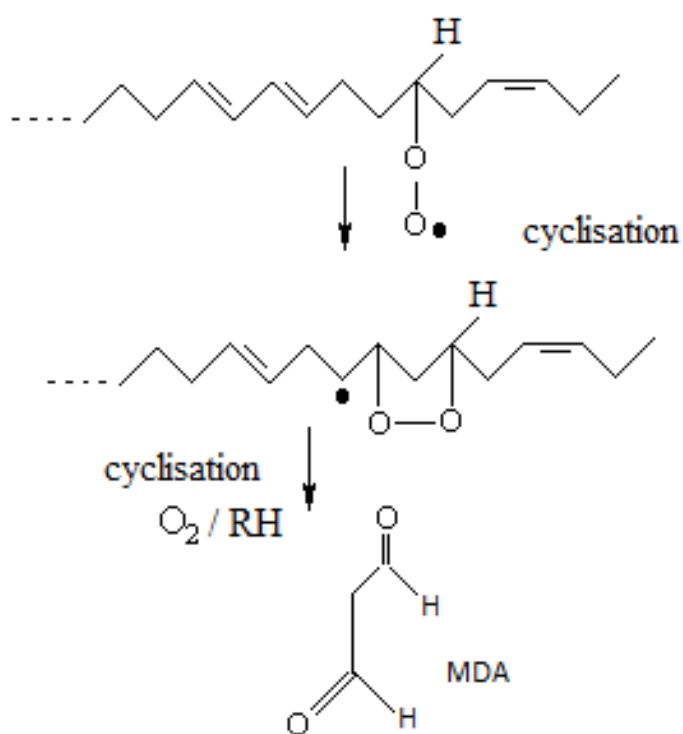
Lipids, usually polyunsaturated fatty acids react with the produced hydroxyl radicals by hydrogen abstraction leading to the formation of lipid free radicals, according to the reaction [4]:



Peroxidized lipids decompose easily, generating both free and core aldehydes and ketones according to the reaction [9] (Mamarelis et.al. 2010).



These reactions explain the FT-IR spectra of coronary and carotid artery. In the region of 1800-1600 cm^{-1} , the band at 1735 cm^{-1} which was assigned to the carbonyl group of lipid esters and the presence of malonaldehyde is confirmed by the former reactions. Malondialdehyde (MDA) is frequently measured as indicator of lipid peroxidation and oxidative stress (Dotan et al., 2004). It is produced from lipid hydroperoxyl radical due to the following reactions:



The non-destructive nature of FT-IR spectroscopy and the ability to directly probe biochemical changes lead to an understanding of the biochemical and structural changes associated with arteriosclerosis. The decrease in the intensity of the band at 1651 cm^{-1} and

the shifting to lower wavenumber (approximately 1630cm^{-1}) justify the way of disappearance of the Amide I band and the change in the structure of proteins from α -helix to random coil due to free radicals reactions.

The bands at the region $1280 - 1170\text{ cm}^{-1}$ are attributed to the presence of O-C-C, O-C(O)-C groups due to the peroxidation of membranes. Thus, the presence of characteristic bands in the region $4000 - 400\text{ cm}^{-1}$ confirms the peroxidation of membranes.

6. Conclusions

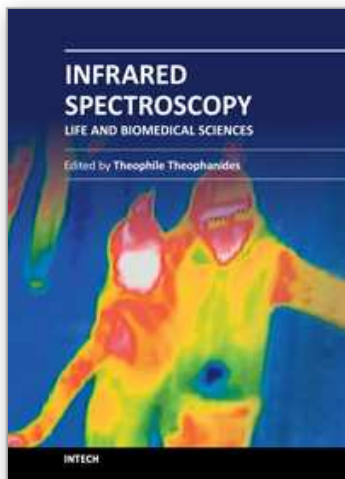
FT-IR spectra showed that hyperoxidation of lipids, phospholipids and membranes take place during atherogenesis. The plaque formation and the increase of LDL lead to change of tertiary structure of proteins from α -helix to random one. FT-IR spectra clearly revealed prominent spectral features corresponding to plaque constituents such as the presence of lipids, lipid esters, fibrous tissues and phosphate group (calcification). Spectral data were correlated well with patients' analyses. The present work demonstrates that infrared spectroscopy can be used to accurately estimate the chemical composition of coronary and carotid arteries. In vivo information about the chemical composition of atherosclerotic lesions may provide a powerful method to detect and characterize sites of atherosclerosis.

7. References

- Anastassopoulou, J., Boukaki, E., Conti, C., Ferraris, P., Giorgini, E., Rubini, C., Sabbatini, S., Theophanides, T. & Tosi, G. (2009). Microimaging FT-IR spectroscopy on pathological breast tissues. *Vibrational Spectroscopy*, Vol. 51, pp.270-275
- Anastassopoulou, J. & Dovas, A. (2007). *Metal ions and cancer*. In S Missailidis(Ed.), The cancer Clock. John Wiley, pp. 27-49
- Anastassopoulou, J. & TheophanidesT.(1990). Raman studies of model vesicle systems. *J Appl Spectrosc*. Vol. 44, pp. 523-525
- Arrondo, J.L.R. & Goni, F.M. (1998). Infrared studies of protein-induced perturbation of lipids in lipoproteins and membranes. *Chemistry and Physics of Lipids*, Vol. 96, pp. 53-68
- Blout, E. R., & Mellors, R. C. (1949). Infrared Spectra of Tissues. *Science*, Vol. 110, pp.137-138
- Barth, A. (2007).Infrared spectroscopy of proteins. *Biochimica et Biophysica Acta*,Vol. 1767, No.9, pp. 1073-101
- Bolanos-Garcia, V.C. & Miguel, R.N. (2003). On the structure and function of apolipoproteins: more than a family of lipid binding proteins. *Progress in Biophysics and Molecular Biology*, Vol. 83, pp. 47-68
- Chua-anusorn, W. & Webb, J. (2000). Infrared spectroscopic studies of nanoscale iron oxide deposits isolated from human thalassemic tissues. *Journal of Inorganic Biochemistry*, Vol. 79, pp.303-309
- Conti, C., Ferraris, P., Giorgini, E., Rubini, C., Sabbatini, S., Tosi, G., Anastassopoulou, J., Arapantoni, P., Boukaki, E., Theophanides, T. & Valavanis, C. (2008). FT-IR Microimaging Spectroscopy:Discrimination between healthy and neoplastic human colon tissues. *Journal of Molecular Structure*, Vol. 881, pp. 46-51
- Deleris, G. & Petibois, C. (2003). Applications of FT-IR spectrometry to plasma contents analysis and monitoring. *Vibrational Spectroscopy*, Vol. 32, pp.129-136

- Dotan, Y., Lichtenberg, D. & Pinchuk, I. (2004). Lipid peroxidation cannot be used as a universal criterion of oxidative stress. *Progress in Lipid Research*, Vol. 43, No. 3, pp. 200-227
- Elliot, A. & Ambrose, E. (1950). Structure of Synthetic Polypeptides. *Nature*, Vol. 165, pp. 921
- Fahrenfort, J. (1961). Attenuated total reflection: A new principle for the production of useful infra-red reflection spectra of organic compound. *Spectrochimica Acta*, Vol. 17, pp. 698-709
- Gazi, E., Dwyer, J., Gardner, P., Ghanbari-Siakhani, A., Wde, A.P., Lockyer, N.P., Vickerman, J.C., Clarke, N.W., Shanks, J.H., Scott, L.J., Hart, C.A. & Brown, M. (2003). Applications of Fourier transform infrared microspectroscopy in studies of benign prostate and prostate cancer. A pilot study. *Journal of Pathology*, Vol. 201, pp. 99-108
- Gorelick, P.B. (2008). Lipoprotein-Associated Phospholipase A2 and Risk of Stroke. *American Journal of Cardiology*, Vol. 101, pp. 34-40
- Goormaghtigh, E., Raussens, V. & Ruysschaert, J.-M. (1999). Attenuated total reflection infrared spectroscopy of proteins and lipids in biological membranes. *Biochimica et Biophysica Acta*, Vol. 1422, pp. 105-185
- Gough, K. M., Zelinski, D., Wiens, R., Rakand, M. & Dixon, M.C. (2003). Fourier transform infrared evaluation of microscopic scarring in the cardiomyopathic heart: Effect of chronic AT1 suppression. *Analytical Biochemistry*, Vol. 316, pp. 232-242
- Halliwell, B. & Gutteridge, J.M.C. (2000). Free radicals in biology and medicine, 3rd ed. London: Oxford University Press, Oxford, UK
- Harrick, N.J. (1960). Study of Physics and Chemistry of Surfaces from Frustrated Total Internal Reflections. *Physical Reviews Letters*, Vol. 4, pp. 224-226
- Insull, W. (2009). The Pathology of Atherosclerosis: Plaque Development and Plaque Responses to Medical Treatment. *The American Journal of Medicine*, Vol. 122, No 1A, pp. S3-S14
- Kamari, Y., Cohen, H., Shaish, A., Bitzur, R., Afek, A., Shen, S., Vainshtein, A. & Harats, D. (2008). Characterisation of atherosclerotic lesions with scanning electron microscopy (SEM) of wet tissue. *Diabetes and Vascular Disease Research*, Vol. 5, 44-47
- Kolovou, P. & Anastassopoulou, J. (2007). Synchrotron FT-IR spectroscopy of human bones. The effect of aging. In: *Brilliant Light in Life and Material Sciences*, V. Tsakanov and H. Wiedemann (Eds.), pp. 267-272., Springer
- Krilov, D., Balarin, M., Kosovic, M., Gamulin, O. & Brnjac-Kraljevic, J. (2009). FT-IR spectroscopy of lipoproteins—A comparative study. *Spectrochimica Acta Part A*, Vol. 73, pp. 701-706.
- Lee, R. T. & Libby, P. (1997). The Unstable Atheroma. *Arteriosclerosis, Thrombosis, and Vascular Biology*, Vol. 17, pp. 1859-1867.
- Legal, J.M., Manfait, M. & Theohaniides, T. (1991). Applications of FTIR spectroscopy in structural studies of cells and bacteria. *Journal of Molecular structure*, Vol. 242, pp. 397-407
- Li, X., Lin, J., Ding, J., Wang, S., Liu, Q. & Qing, S. (2004). Raman spectroscopy and fluorescence for the detection of liver cancer and abnormal liver tissue, *Annual Inter Conf IEEE EMBS*, San Francisco, September 1-5, 2004
- Liu, K.Z., Bose, R. & Mantsch, H.H. (2002). Infrared spectroscopic study of diabetic platelets. *Vibrational Spectroscopy*, Vol. 28, pp. 131-136

- Mamarelis, I., Pissaridi, K., Dritsa, V., Kotileas, P., Tsiligiris, V., Tzilalis, V. & Anastassopoulou, J. (2010). Oxidative stress and atherogenesis. An FT-IR spectroscopic study. *In Vivo*, Vol. 24, pp.883-888
- McIntosh, L.M., Jackson, M., Mantsch, H., Stranc, M.F. , Pilavdzic, D. & Crowson, A.N.(1999) Infrared Spectra of Basal Cell Carcinomas are Distinct from Non-Tumor-Bearing Skin Components. *Journal of Investigative Dermatology*, Vol. 112, pp. 951-956.
- Nara, M., Okazaki, M., & Kagi, H. (2002). Infrared study of human serum very-low-density and low-density lipoproteins. Implication of esterified lipid C-O stretching bands for characterizing lipoproteins. *Chemistry and Physics of Lipids*, Vol. 117, pp. 1-6.
- Petra, M., Anastassopoulou, J., Theologis, T. & Theophanides T. (2005). Synchrotron micro-FT-IR spectroscopic evaluation of normal paediatric human bone. *Journal of Molecular Structure*, Vol. 78, pp. 101-116
- Parthasarathy, S., Litvinov, D., Selvarajan, K. & Garelnabi M. (2008).Lipid peroxidation and decomposition – Conflicting roles in plaque vulnerability and stability. *Biochimica et Biophysica Acta*, Vol. 1781, pp. 221-231
- Ross, R. & Glomset, J. A. (1973). Atherosclerosis and the arterial smooth muscle cell. *Science* Vol. 180, pp. 1332-1339
- Stary, H.C. (2000). Natural history and histological classification of atherosclerotic lesions: an update. *Arteriosclerosis, Thrombosis, and Vascular Biology*, Vol. 20, pp. 1177-1178
- Steinberg, D. & Witztum, J.L. (1990). Lipoproteins and atherogenesis. *Journal of American Medical association* . Vol. 264, pp. 3047-3052
- Theophanides, T., Angibust, J.P. & Manfait M. (1988). *Protein and Nucleic Acid Changes*. In Twardowski (Ed.), *Spectroscopic and Structural Studies of Biomaterials, I. Proteins*, Sigma Press, Wilmslow, UK, pp. 3-14
- Theophanides, T. (1984). *Fourier Transform Infrared Spectroscopy*. D. Reidel Publishing Co., Dodrecht.
- Theophanides, T. (1978). *Infrared and Raman spectroscopy of biological molecules*. NATO Advanced Study Institute, D Reidel Publishing Co, Dodrecht
- Woernley, D. L. (1952). Infrared Absorption Curves for Normal and Neoplastic Tissues and Related Biological Substances. *Cancer Research*, Vol. 12, pp. 516
- Yano, K., Ohoshima, S., Gotou, Y., Kumaido, K., Moriguchi, T. & Katayama H. (2000). Direct Measurement of Human Lung Cancerous and Noncancerous Tissues by Fourier Transform Infrared Microscopy: Can an Infrared Microscope Be Used as a Clinical Tool? *Analytical Biochemistry*, Vol. 287, pp. 218-225



Infrared Spectroscopy - Life and Biomedical Sciences

Edited by Prof. Theophanides Theophile

ISBN 978-953-51-0538-1

Hard cover, 368 pages

Publisher InTech

Published online 25, April, 2012

Published in print edition April, 2012

This informative and state-of-the art book on Infrared Spectroscopy in Life sciences designed for researchers, academics as well as for those working in industry, agriculture and in pharmaceutical companies features 20 chapters of applications of MIRS and NIRS in brain activity and clinical research. It shows excellent FT-IR spectra of breast tissues, atheromatic plaques, human bones and projects assessment of haemodynamic activation in the cerebral cortex, brain oxygenation studies and many interesting insights from a medical perspective.

How to reference

In order to correctly reference this scholarly work, feel free to copy and paste the following:

Vasiliki Dritsa (2012). FT-IR Spectroscopy in Medicine, Infrared Spectroscopy - Life and Biomedical Sciences, Prof. Theophanides Theophile (Ed.), ISBN: 978-953-51-0538-1, InTech, Available from:
<http://www.intechopen.com/books/infrared-spectroscopy-life-and-biomedical-sciences/ft-ir-spectroscopy-in-medicine>

INTECH
open science | open minds

InTech Europe

University Campus STeP Ri
Slavka Krautzeka 83/A
51000 Rijeka, Croatia
Phone: +385 (51) 770 447
Fax: +385 (51) 686 166
www.intechopen.com

InTech China

Unit 405, Office Block, Hotel Equatorial Shanghai
No.65, Yan An Road (West), Shanghai, 200040, China
中国上海市延安西路65号上海国际贵都大饭店办公楼405单元
Phone: +86-21-62489820
Fax: +86-21-62489821

© 2012 The Author(s). Licensee IntechOpen. This is an open access article distributed under the terms of the [Creative Commons Attribution 3.0 License](https://creativecommons.org/licenses/by/3.0/), which permits unrestricted use, distribution, and reproduction in any medium, provided the original work is properly cited.

IntechOpen

IntechOpen